Nuclear Instruments and Methods in Physics Research B 267 (2009) 872–875

Contents lists available at ScienceDirect

Nuclear Instruments and Methods in Physics Research B

journal homepage: www.elsevier.com/locate/nimb

Calculated energy loss of a swift fullerene ion beam in InP

Isabel Abril [a], Rafael Garcia-Molina [b], Cristian D. Denton [a,*], Santiago Heredia-Avalos [c]

[a] Departament de Física Aplicada, Universitat d'Alacant, Apartat 99, E-03080 Alacant, Spain
[b] Departamento de Física – CIOyN, Universidad de Murcia, Apartado 4021, E-30080 Murcia, Spain
[c] Departament de Física, Enginyeria de Sistemes i Teoria del Senyal, Universitat d'Alacant, Apartat 99, E-03080 Alacant, Spain

ARTICLE INFO

Available online 11 February 2009

PACS:
34.50.Bw
36.40.−c
61.48.+c

Keywords:
Energy loss
Stopping power
Clusters
Vicinage effects
Fullerene

ABSTRACT

Bombardment of semiconductors with fullerene has been used to induce the formation of tracks. It is now accepted that target electronic excitation and ionization, which gives rise to the slowing down of the projectile is essential to calculate the track diameter. In the case of cluster beams, like fullerenes, the electronic excitation induced by each of the cluster constituents is enhanced, for certain projectile energies and target depths, by the so-called vicinage effects. Here we use a simulation code to calculate the energy lost by a swift fullerene ion beam in InP, paying special attention to the vicinage effects where they are significative. The code describes classically the movement of each cluster constituent under the influence of the self-retarding force, the Coulomb repulsion among molecular fragments, the wake forces responsible for the vicinage effects and the multiple scattering with the target nuclei. The simulation code also takes into account the possibility that the molecular fragments can also capture or loss electrons from the target, changing its charge state in their travel through the solid.

Our simulations show that the energy deposited by the atomic ions that constitute the C_{60} ion is clearly higher than the energy deposited by the same atomic ions but isolated. This difference being larger as the incident energy increases. We have predicted that track diameters of ~ 244 Å can be obtained in an InP target when using C_{60} ions with an initial energy of 300 MeV.

© 2009 Elsevier B.V. All rights reserved.

The study of tracks formation with swift heavy ions or cluster ions in materials is interesting for applications in nano-devices [1–3] and also in order to understand the physical phenomena implied in the interaction of both atomic and molecular ions with solids. Irradiation experiments with swift heavy ions have shown stable defects or tracks formation induced in metals, conductive oxides or insulators; besides, the size of these tracks has been studied for a large number of incident ions and energies that involve high values of the energy in electronic excitations [4–6]. However, in most cases the bombardment of semiconductors with swift heavy ions did not show tracks formation, even when using high energy heavy ion accelerators to reach a high deposited electronic energy in the target [7–9]. This behaviour implies that it is necessary a higher deposited energy in semiconductors than in insulators.

The recent availability of accelerated cluster beams has made possible to reach higher densities of deposited energy than those obtained with swift heavy ions [10]. In these conditions tracks formation has been reported by the bombardment of fullerene ion beams, with a total energy of tens of MeV, in several semiconductors such as Si, Ge, GaAs or InP [11–14]. This fact can be explained considering the high density of the deposited electronic energy reached with swift C_{60} ions as compared with those obtained with swift heavy ions.

The aim of this work is to calculate the energy deposited by a fullerene ion beam in an InP target, as a function of its incident energy and the depth in the target, in order to find out the conditions for the highest deposited energy in the target. We choose an InP target due to its interesting electronic properties (it has been extensively used in optoelectronic and high power microwave devices, as well as in telecommunication applications [15]), and also because there are recent experimental measurements for this projectile-target combination [14].

Current theories about the size of the tracks formation such as the thermal spike model (TSM) [16], assume that when a swift ion moves through a solid a high temperature region is formed around the trajectory of the ion, which produces a track. The radius of this track depends on the electronic energy loss of the incident ion and on a threshold electronic energy loss required for the track formation. Therefore, in order to predict the size of the track a model to evaluate the electronic energy loss is necessary.

When a swift C_{60} ion impinges on an InP target, it dissociates in the first atomic layers of the solid and moves through the target with a certain correlated initial spatial distribution. These constituents (atomic ions or fragments) suffer electronic capture and loss

* Corresponding author.
E-mail address: denton@ua.es (C.D. Denton).

0168-583X/$ - see front matter © 2009 Elsevier B.V. All rights reserved.
doi:10.1016/j.nimb.2009.02.042

processes changing their charge state in their travel through the target, until they reach a dynamical equilibrium charge state. During their motion through the solid the fragments lose energy due to excitations of the target electrons and nuclear scattering with the target atoms. Moreover, each fragment interacts with its partners through the wake forces and the Coulomb repulsion [17,18]. As a consequence of the wake forces, the energy loss of the carbon atomic ions resulting from the dissociation of the C_{60} cluster can be different than the energy loss of the same, but isolated, carbon atomic ions, giving rise to the so-called vicinage effects in the energy loss [17,18].

We calculate the energy loss of a fullerene ion beam on an InP target by using a simulation code that is based in a combination of molecular dynamics and Monte Carlo techniques [17,18]. Our simulation code uses a finite difference algorithm to numerically calculate the trajectories of all the fragments resulting from the dissociation of the incident fullerene ion; for this purpose, it includes in a realistic manner all the interactions previously cited. The code also considers the fact that the incident C_{60} bombards the target randomly oriented with respect to the beam direction. We summarize in the following the model used in our simulation code to describe the inelastic electronic energy loss of the projectile.

When the i-atomic ion (with atomic number Z_i) is moving with velocity v_i through a solid characterized by the energy-loss function (ELF) $\mathrm{Im}[-1/\epsilon(k,\omega)]$, it is slowed down by losing energy in electronic excitations of the target (with transferred energy and momentum $\hbar\omega$ and $\hbar k$, respectively). The target electronic excitations are characterized by its dielectric function $\epsilon(k,\omega)$. The projectile slowing down is described by the stopping power, $S_{p,i}$, and the energy-loss straggling, Ω_i^2, which, in the dielectric formalism, are given by

$$S_{p,i} = \frac{2e^2}{\pi v_i^2}\int_0^\infty \mathrm{d}k \frac{[Z_i-\rho_i(k)]^2}{k}\int_0^{kv_i}\mathrm{d}\omega\,\omega\mathrm{Im}\left[\frac{-1}{\epsilon(k,\omega)}\right], \quad (1)$$

$$\Omega_i^2 = \frac{2e^2\hbar}{\pi v_i^2}\int_0^\infty \mathrm{d}k \frac{[Z_i-\rho_i(k)]^2}{k}\int_0^{kv_i}\mathrm{d}\omega\,\omega^2\mathrm{Im}\left[\frac{-1}{\epsilon(k,\omega)}\right], \quad (2)$$

where $\rho_i(k)$ is the Fourier transform of the electronic density of the i-atomic ion, which depends on its charge state q. The stopping force that acts on the i-atomic ion fluctuates because the stochastic nature of the interaction with the target electrons. So the modulus of the stopping force is given by a Gaussian distribution, for which $S_{p,i}$ is the mean value and $\Omega_i/\sqrt{\Delta d_i}$ is the standard deviation, with $\Delta d_i = v_i\Delta t$ being the distance travelled by this atomic ion in a time step Δt.

The Fourier transform of the electronic charge density $\rho_i(k)$ of the i-atomic fragment can be obtained (for medium size ions, like carbon) from the statistical Brandt–Kitagawa model [19]. On the other hand, the electronic properties of the InP target are described by the MELF-GOS model [20,21], where $\mathrm{Im}\,[-1/\epsilon(k,\omega)]$ is obtained by combining a sum of Mermin-type [22] energy-loss functions that fits to experimental optical data, and the use of generalized oscillator strengths. These contributions account for excitations of the target outer-shell and inner-shell electrons, respectively [20,21].

In Fig. 1 we depict the average stopping force for carbon atomic ions moving through an InP target, see Eq. (1), evaluated as the weighted sum of the stopping forces for the different equilibrium charge states of the projectile. We use the equilibrium charge fractions provided by a fit to experimental data [23]. The solid curve represents our calculations, whereas the dashed curve is the semi-empirical prediction provided by the SRIM-2008 code [24], which is based on fits to experimental stopping cross sections (SCS). There are remarkable discrepancies ($\sim 40\%$ around the maximum of the SCS) between our results and those provided by the SRIM-2008 code. These differences could be explained by the following two

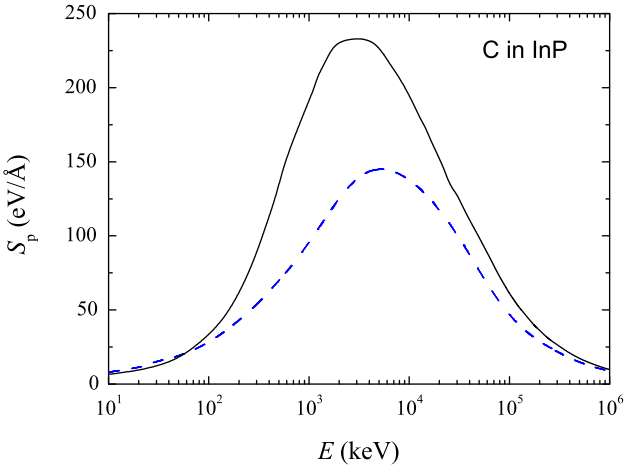

Fig. 1. Average stopping force for carbon atomic ions incident on InP, as a function of the projectile energy. The solid curve represents our calculations, whereas the dashed curve is the result obtained using the SRIM-2008 code [24].

reasons. Firstly, when there are not experimental SCS measurements for the compound target, the corresponding predictions by the SRIM-2008 code are obtained from the application of Bragg rule to the SCS of each target constituent, neglecting chemical effects. On the contrary, our model takes into account the chemical effects because the low-energy region of the ELF, which mainly describes the valence band excitations, is properly fitted to the experimental optical ELF of the compound target [21]. Secondly, our model is based on the dielectric formalism, which assumes a linear response of the target electrons to the perturbation induced by the projectile, neglecting higher-order effects. This formalism loses validity as the projectile atomic number increases and its energy decreases. In these situations non-linear effects, such as the Bloch and Barkas corrections [25], become more significant. According to simple estimates, obtained using the computer code HISTOP [26], non-linear effects tend to increase the linear SCS for small charge states of the projectile, as it is in our case. They can represent 9% of the SCS around the SCS maximum. Therefore the main differences between our results and the SRIM-2008 code should be attributed to the proper inclusion of the chemical effects. Unfortunately, there are not experimental data to compare with in order to elucidate the proportion in which chemical and non-linear effects could explain these differences, although it is worth to mention that we have recently calculated the stopping force for hydrogen and helium projectiles moving through an InP target with this model and we have obtained a good agreement with the available experimental data [27].

The wake force must be understood as a force due to the electronic density induced in the medium by a swift fragment which affects the neighbor fragments. In the dielectric formalism, the wake force exerted by a j-fragment on a i-fragment is located in the plane defined by the position of both fragments and the velocity of the j-fragment. Using cylindrical coordinates, the wake force acting on the i-fragment due to its neighbor, denoted by j, can be decomposed into its parallel and perpendicular components with respect to the velocity $\mathbf{v}_j$,

$$F_{\parallel ij} = \frac{2}{\pi v_j^2}\int_0^\infty \frac{\mathrm{d}k}{k}[Z_i-\rho_i(k)]\left[Z_j-\rho_j(k)\right] \times \int_0^{kv_j}\mathrm{d}\omega\omega\, J_0\left(R_{\perp ij}\sqrt{k^2-\omega^2/v_j^2}\right) \times\left\{\sin\left(\frac{\omega R_{\parallel ij}}{v_j}\right)\mathrm{Re}\left[\frac{1}{\epsilon(k,\omega)}-1\right]+\cos\left(\frac{\omega R_{\parallel ij}}{v_j}\right)\mathrm{Im}\left[\frac{1}{\epsilon(k,\omega)}\right]\right\}, \quad (3)$$

and

$$F_{\perp ij} = \frac{2}{\pi v_j}\int_0^\infty \frac{dk}{k}[Z_i - \rho_i(k)]\left[Z_j - \rho_j(k)\right] \times \int_0^{kv_j} d\omega \sqrt{k^2 - \omega^2/v_j^2}\, J_1\left(R_{\perp ij}\sqrt{k^2 - \omega^2/v_j^2}\right) \times \left\{\cos\left(\frac{\omega R_{\parallel ij}}{v_j}\right)\mathrm{Re}\left[\frac{1}{\epsilon(k,\omega)} - 1\right] - \sin\left(\frac{\omega R_{\parallel ij}}{v_j}\right)\mathrm{Im}\left[\frac{1}{\epsilon(k,\omega)}\right]\right\}, \quad (4)$$

where $R_{\parallel ij}$ and $R_{\perp ij}$ are the relative distances between the i- and j-fragments in the direction parallel and perpendicular, respectively, to the movement of the j-fragment; J_0 and J_1 are Bessel functions of the first kind.

We show in Fig. 2 the parallel and perpendicular components of the wake forces, $F_\parallel$ and $F_\perp$, that act on a C^{3+} ion (partner ion) due to another C^{4+} ion (leading ion, located at the origin of the coordinates in the graph) as a function of the distance $R_\parallel$, both moving with an energy of 3 MeV through an InP target. We choose this particular case, because the equilibrium charge state for this projectile energy is comprised between +3 and +4. Note that the general trend of the wake force is to reduce the Coulomb repulsion between the partner fragments, giving rise to a higher density of the energy deposited on the target. In fact the negative values of $F_\perp$ tend to align the partner ions, whereas the positive values of $F_\parallel$ behind the leading ion tend to move closer the partner ions in the beam direction, both reducing the Coulomb repulsion and giving rise to a high deposited energy in the target [28,29].

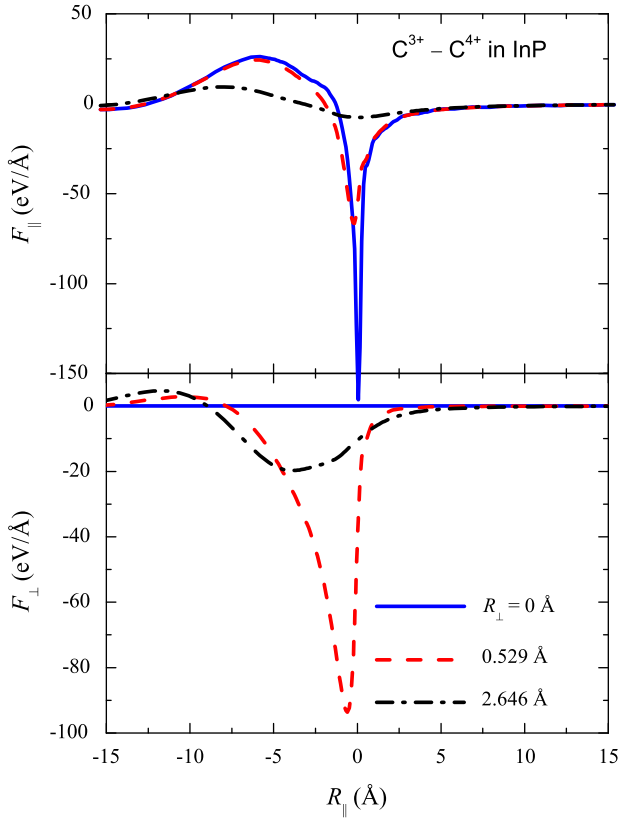

Fig. 2. Parallel and perpendicular components of the wake forces that act on a C^{3+} ion due to a neighbor C^{4+} ion (located at the origin of the graph, $R_\parallel = 0$, and moving from left to right), as a function of the parallel component $R_\parallel$ of the interatomic distance; both ions moving with $E = 3$ MeV through an InP target. We show results for several perpendicular distances $R_\perp$ between the C^{+3} and C^{+4}.

On the other hand, the interactions between the fragments of the cluster and the target nuclei are the main responsible of the angular spread of the fragments. We include the multiple elastic scattering with the target nuclei in our simulation code via a Monte Carlo algorithm. More details about the models we use to describe the elastic multiple scattering of the dissociated fragments with the target nuclei and the capture and loss of electrons by the dissociated atomic ions can be found in [17].

Considering all these ingredients, our simulation code allows us to follow the trajectories of each cluster fragment and to know at each time their position and velocity. Therefore, we can evaluate the energy lost by the fullerene beam when moving through the InP target.

In order to obtain the energy deposited on an InP target, we have evaluated the energy lost by the carbon atomic ions resulting from the dissociation of the C_{60} ion when moving through the InP target. The differences between the energy deposited by the C_{60} ion and the sum of the energy deposited by each one of its constituents moving with the same velocity but isolated are quantified through the instantaneous stopping ratio

$$\mathscr{R} = \frac{\Delta E(C_{60}^+)}{60 \cdot \Delta E(C^+)}, \quad (5)$$

where $\Delta E(C_{60}^+)$ is the energy deposited by a C_{60}^+ projectile in a given depth D when it impinges on the target with an initial charge state $q = +1$; analogously for $\Delta E(C^+)$, which is the energy deposited by a C^+ projectile. As previously stated, our simulation code takes into account that the projectiles change its charge state during its travel through the target due to electronic capture and loss processes, so the calculation of $\mathscr{R}$ also considers the evolution of the projectile charge state.

In Fig. 3 we depict the instantaneous stopping ratio $\mathscr{R}$ as a function of the target depth for different projectile initial energies. The labels inside the figure indicate the incident energy in MeV of the C_{60} ion. Note that $\mathscr{R} > 1$ for almost all incident energies, although this trend is not satisfied for the smaller depths, where $\mathscr{R} < 1$. This is more noticeable for low initial energies and it is due to the different initial charge states of the C^+ as compared to those of the dissociated atomic ions (59 C^0 atoms and 1 C^+ ion). In addition, $\mathscr{R}$ tends to unity when the depth inside the target increases. Such behaviour is due to two factors that increase the interatomic distances (i.e. the nuclear scattering and the Coulomb repulsion), resulting in the extinction of the vicinage effect.

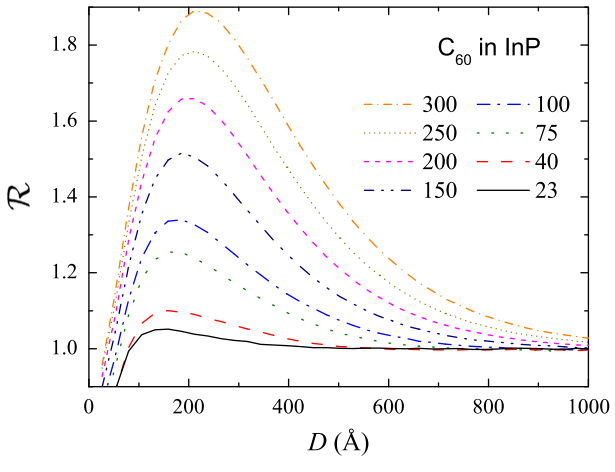

Fig. 3. Instantaneous stopping ratio $\mathscr{R}$ for C_{60} ions with different energies incident on an InP target, as a function of the target depth. The labels indicate the total incident energy in MeV of the C_{60} ion.

According to Fig. 3 a carbon atom of the fullerene projectile deposits higher energy (as compared with the energy deposited by the same carbon atom but isolated) when its incident energy increases. For instance, the energy deposited by a C_{60} ion with $E = 150$ MeV is almost ~ 1.5 times the energy deposited by 60 individual C^+ ions with the same incident energy. Therefore, in order to increase the radius of the track, projectiles with higher incident energy should be used. There is a theoretical limit for $\mathscr{R}$ stated by the closeness between the atoms that constitute the cluster and by their atomic number Z_i. Specifically, $\mathscr{R}$ increases when the atoms that form the cluster are closer each other and when they have higher atomic number. We have estimated such limit using the united-atom model stated in [30]. According to this model, the stopping power for a cluster constituted by n atoms with atomic number Z_i is given by the corresponding stopping power for an united-atom with atomic number $n \cdot Z_i$; so we obtain $\mathscr{R} \leqslant 60$ for a C_{60}^+ projectile, which is an unattainable limit for usual projectile incident energies. For instance, using the analytical procedure provided in [31], we have estimated $\mathscr{R} \lesssim 6.3$ for a C_{60}^+ projectile incident with $E = 60$ MeV/atom on an InP target.

In the thermal spike model (TSM) [16], the track radius R_0 is given by the relation

$$R_0^2 = \frac{a_0^2}{2.7}\frac{\Delta E}{\Delta E_{\mathrm{th}}}, \tag{6}$$

where $a_0 = 79.5$ Å, ΔE is the electronic energy loss of the incident fullerene ion, and ΔE_{th} is the threshold electronic energy loss required for track formation. In this particular case, we assume $\Delta E_{\mathrm{th}} \simeq 1347$ eV/Å , as stated in [14]. It is worth to mention that the previous equation is only applicable when $\Delta E > 2.7\Delta E_{\mathrm{th}}$, condition that is satisfied in all cases we consider in this work.

Recently, Dhamodaran et al. [14] have observed that track diameters resulting from Eq. (6), which neglects the effect of the wake forces in the energy deposited by the cluster, are not consistent with their experiments. Specifically, the theoretical track radii are about twice smaller than the experimental ones; for instance, they obtained $R_0 \simeq 54$ Å for fullerene ions with an initial energy of 40 MeV, whereas the experimental result was $R_0 \simeq 103$ Å. On the other hand, our simulation code provides $R_0 \simeq 80$ Å for such experimental situation (where $\mathscr{R} \sim 1$), in better agreement with the experimental data. This significant improvement can be explained according to Fig. 1, because the electronic stopping force derived from Eq. (1) is higher than the results provided by the SRIM-2008 semiempirical code [24], giving rise to higher values of ΔE.

Additionally, our simulation code, which includes wake forces, predicts that the inelastic electronic energy loss of C_{60} ions is higher than that obtained for 60 isolated C^+ ions, specially for high projectile initial energies, so the corresponding track radius should be in this situations even larger. For instance, the energy deposited at $D \sim 200$ Å in an InP target by a C_{60} cluster, with an initial energy of 300 MeV, can be almost twice the energy deposited by 60 isolated C^+ ions. Therefore, we obtain for this situation $R_0 = 122$ Å, according to Eq. (6).

In summary, we have calculated the energy deposited in an InP irradiated by swift C_{60} ions as a function of the incident energy. In order to make these calculations we have used a simulation code previously developed by our group [17,18], which is based on a combination of molecular dynamics and Monte Carlo techniques. The simulation code considers that the carbon atomic ions resulting from the dissociation of the C_{60} ion feel Coulomb repulsion, stopping, and wake forces, and suffers capture and loss of electrons and nuclear scattering with the target nuclei.

We have obtained that the projectile deposits higher density of energy as its incident energy increases, so in order to induce track formation, projectiles with high incident energy should be used. Although our simulations predicts an increase of the track diameters compared to those obtained when vicinage effects in the energy loss are not considered, they are still quantitatively inconsistent with the experimental data [14], so an improvement concerning the TSM used to relate the track diameter with the electronic energy lost by the projectile on the target should be make.

Acknowledgement

This work has been financially supported by the Spanish Ministerio de Ciencia e Innovación (Projects Nos. FIS2006-13309-C02-01 and FIS2006-13309-C02-02). CDD thanks the Spanish Ministerio de Ciencia e Innovación and Generalitat Valenciana for support under the Ramón y Cajal Program. We acknowledge useful discussions with Néstor R. Arista.

References

[1] H. Dammak, A. Weidinger, Nucl. Instr. and Meth. B 146 (1998) 285.
[2] W. Wesch, A. Kamarou, E. Wendler, Nucl. Instr. and Meth. B 225 (2004) 111.
[3] J.H. Zollondz, A. Weidinger, Nucl. Instr. and Meth. B 225 (2004) 178.
[4] B. Canut, S.M.M. Ramos, P. Thevenard, N. Marceffu, A. Benyagoub, G. Marest, A. Meftah, M. Toulemonde, F. Studer, Nucl. Instr. and Meth. B 80–81 (1993) 1114.
[5] H. Dammak, A. Dunlop, D. Lesueur, Nucl. Instr. and Meth. B 107 (1996) 204.
[6] S. Hémon, C. Dufour, A. Berthelot, F. Gourbilleau, E. Paumier, J. Gégin-Collin, Nucl. Instr. and Meth. B 166 (2000) 339.
[7] M. Mikou, R. Carin, P. Bogdanski, R. Madelon, Nucl. Instr. and Meth. B 107 (1996) 246.
[8] M. Levalois, P. Marie, Nucl. Instr. and Meth. B 156 (1999) 64.
[9] W. Wesch, A. Kamarou, E. Wendler, A. Undisz, M. Rettenmayr, Nucl. Instr. and Meth. B 257 (2007) 283.
[10] S. Della-Negra, A. Brunelle, Y. Le Beyec, J.M. Curaudeau, J.P. Mouffron, B. Waast, P. Hakansson, B.U.R. Sundqvist, E. Parilis, Nucl. Instr. and Meth. B 74 (1994) 453.
[11] A. Dunlop, G. Jaskierowicz, S. Della-Negra, Nucl. Instr. and Meth. B 146 (1998) 302.
[12] A. Colder, O. Marty, B. Canut, M. Levalois, P. Marie, X. Portier, S.M.M. Ramos, M. Toulemonde, Nucl. Instr. and Meth. B 174 (2001) 491.
[13] A. Colder, B. Canut, M. Levalois, P. Marie, X. Portier, S.M.M. Ramos, J. Appl. Phys. 91 (2002) 5853.
[14] S. Dhamodaran, A.P. Pathak, A. Dunlop, G. Jaskierowicz, S. DellaNegra, Nucl. Instr. and Meth. B 256 (2007) 229.
[15] O. Wada, H. Hasegawa, InP-based Materials and Devices: Physics and Technology, John Wiley & Sons, New York, 1994.
[16] G. Szenes, Z.E. Horvath, B. Pecz, F. Paszti, L. Toth, Phys. Rev. B 65 (2002) 045206.
[17] S. Heredia-Avalos, R. Garcia-Molina, I. Abril, Phys. Rev. A 75 (2007) 012901.
[18] S. Heredia-Avalos, I. Abril, C.D. Denton, R. Garcia-Molina, Phys. Rev. A 76 (2007) 012901.
[19] W. Brandt, M. Kitagawa, Phys. Rev. B 25 (1982) 5631.
[20] I. Abril, R. Garcia-Molina, C.D. Denton, F.J. Pérez-Pérez, N.R. Arista, Phys. Rev. A 58 (1998) 357.
[21] S. Heredia-Avalos, R. Garcia-Molina, J.M. Fernández-Varea, I. Abril, Phys. Rev. A 72 (2005) 052902.
[22] N.D. Mermin, Phys. Rev. B1 (1970) 2362.
[23] P.L. Grande, G. Schiwietz, CasP. Convolution Approximation for Swift Particles, Version 3.1, 2004, Code available from <http://www.hmi.de/people/schiwietz/casp.html>.
[24] J.F. Ziegler, J.P. Biersack, SRIM-2008, The Stopping and Range of Ions in Matter, Version 2008, Code available from <http://www.srim.org>.
[25] J.C. Ashley, J. Phys.: Condens. Matter 3 (1991) 2741.
[26] N.R. Arista, Private communication.
[27] S. Heredia-Avalos, J.C. Moreno-Marín, I. Abril, R. Garcia-Molina, Nucl. Instr. and Meth. B 230 (2005) 118.
[28] Y.-N. Wang, H.-T. Qiu, Z.L. Mišković, Phys. Rev. Lett. 85 (2000) 1448.
[29] S. Heredia-Avalos, C.D. Denton, R. Garcia-Molina, I. Abril, Phys Rev. Lett. 88 (2002) 079601.
[30] D. Ben-Hamu, A. Baer, H. Feldman, J. Levin, O. Heber, Z. Amitay, Z. Vager, D. Zajfman, Phys. Rev. A 56 (1997) 4786.
[31] S. Heredia-Avalos, R. Garcia-Molina, Phys. Rev. A 76 (2007) 032902.